Finite volume schemes for elliptic and elliptic-hyperbolic problems on triangular meshes

Raphaèle Herbin and Olivier Labergerie

R.H. : CMI, Université de Provence,
13453 Marseille, France.
O.L. : Institut Français du Pétrole,
BP 311, 92506 Rueil Malmaison, France.

Abstract : We present here a numerical comparison between different finite volume schemes for several equations. An elliptic equation of a diffusion-convection type and an elliptic-hyperbolic coupled system will be considered on an open bounded set Ω of $\mathbb{R}^2$, using a triangular mesh for the discretization of Ω. A four point finite volume scheme (FV) and a "weighted" finite volume scheme (WFV) are presented along with the geometrical assumptions on the mesh. Both schemes are compared in the following cases:

- the pure diffusion operator, for which the WFV scheme may be seen as a finite element scheme with stabilization and numerical integration, and a diffusion-convection operator.
- a hyperbolic equation and a system of elliptic-hyperbolic equations.

In all cases, the performance of both schemes are comparable, and the FV scheme is computationally cheaper.

Keywords : finite volume method, finite element method, diffusion-convection, elliptic-hyperbolic systems of p.d.e's.

AMS Classification : 35A40, 65M60, 65N30.

1 Introduction

Our aim here is to compare a "classical" finite volume scheme and a "weighted" finite volume scheme for the discretization of partial differential equations and systems of p.d.e's, using a triangular mesh. In order to do so, we shall consider two problems, which arise in various engineering fields.
The first one is an elliptic equation which models a diffusion-convection problem :

$$\begin{aligned} -\mathrm{div}(k(\mathbf{x})\nabla u(\mathbf{x})) + \mathrm{div}(u(\mathbf{x})\mathbf{v}(\mathbf{x})) + b(\mathbf{x})u(\mathbf{x}) - f(\mathbf{x}) &= 0, \mathbf{x} \in \Omega, & (1)\\ u(\mathbf{x}) &= g(\mathbf{x}), \mathbf{x} \in \partial\Omega, & (2) \end{aligned}$$

where Ω is an open bounded polygonal set of $\mathbb{R}^2$, k a function from $\overline{\Omega}$ into $\mathbb{R}_+$ of class C^1, such that there exists $\kappa > 0$ such that $k(\mathbf{x}) \geq \kappa$, $\forall \mathbf{x} \in \Omega$, $\mathbf{v}$ a function from $\overline{\Omega}$ to $\mathbb{R}^2$ of class C^1, such that $\mathrm{div}\mathbf{v} \geq 0$, and $f \in C(\overline{\Omega})$, $g \in C(\partial\Omega)$. In the case of a heat transfer problem, u represents the temperature, $-k\nabla u$ is the conductive heat flux and $u\mathbf{v}$ is the convective heat flux.

The second problem is a system of equations which models a two phase flow in a porous medium :

$$
\begin{aligned}
s_t(\mathbf{x},t) - \mathrm{div}(k_1(s(\mathbf{x},t))\nabla p(\mathbf{x},t)) &= f_1(\mathbf{x},t), (\mathbf{x},t) \in \Omega\times]0,\mathrm{T}[, &(3)\\
-s_t(\mathbf{x},t) - \mathrm{div}(k_2(s(\mathbf{x},t))\nabla p(\mathbf{x},t)) &= f_2(\mathbf{x},t), (\mathbf{x},t) \in \Omega\times]0,\mathrm{T}[, &(4)\\
s(\mathbf{x},t) &= s_1(\mathbf{x},t), (\mathbf{x},t) \in \partial\Omega^-\times]0,\mathrm{T}[, &(5)\\
s(\mathbf{x},0) &= s_0(\mathbf{x}), \mathbf{x} \in \Omega, &(6)\\
p(\mathbf{x},t) &= p_1(\mathbf{x},t), (\mathbf{x},t) \in \partial\Omega\times]0,\mathrm{T}[, &(7)\\
p(\mathbf{x},0) &= p_0(\mathbf{x}), \mathbf{x} \in \Omega, &(8)
\end{aligned}
$$

where Ω is an open bounded polygonal set of $\mathbb{R}^2$, k_1 and k_2 are two convex functions from $\mathbb{R}$ into $\mathbb{R}_+$ of class C^1, such that $k_1' \geq 0$ and $k_2' \geq 0$, f_1 and f_2 are two functions of $C^0(\Omega\times]0,\mathrm{T}[,\mathbb{R})$ and $s_1 \in C^2(\partial\Omega^-\times]0,\mathrm{T}[,\mathbb{R})$, $s_0 \in C^2(\Omega,\mathbb{R})$, $u_1 \in C^1(\partial\Omega\times]0,\mathrm{T}[,\mathbb{R})$, $u_0 \in C^1(\Omega,\mathbb{R})$ and $\partial\Omega^- = \{\mathbf{x} \in \partial\Omega \ / \ \nabla u(\mathbf{x},.).\mathbf{n}(\mathbf{x}) \leq 0\}$ with $\mathbf{n}(\mathbf{x})$ the outward normal unit vector to the boundary $\partial\Omega$. In the case of a "petroleum engineering" problem, p represents the pressure, k_1 and k_2 are the phase mobilities and s is the saturation of one of the phases.

Summing Equations (3) and (4) yields an elliptic equation. In the sequel, we shall in fact discretize the following system :

$$
\begin{aligned}
s_t(\mathbf{x},t) - \mathrm{div}(k_1(s(\mathbf{x},t))\nabla p(\mathbf{x},t)) &= f_1(\mathbf{x},t), (\mathbf{x},t) \in \Omega\times]0,\mathrm{T}[, &(9)\\
-\mathrm{div}((k_1+k_2)(s(\mathbf{x},t))\nabla p(\mathbf{x},t)) &= (f_1+f_2)(\mathbf{x},t), (\mathbf{x},t) \in \Omega\times]0,\mathrm{T}[, &(10)
\end{aligned}
$$

with boundary conditions (5)-(8).

Finite volume methods have been extensively used for industrial problems, in the case of hyperbolic equations ([1], [13], [10]), elliptic equations ([6],[7]) or coupled systems of equations ([8], [9], [6], [14]). The advantage of finite volume schemes using triangular meshes is clear for convection diffusion equations. On one hand, the stability and convergence properties of the finite volume scheme (using an upwind choice for the convective flux) ensure a robust scheme for any mesh satisfying the assumptions (11) and (12) stated below, without any need of refinement in the areas of a large convection flux. On the other hand, the use of a triangular mesh allows the computation of a solution for any shape of the physical domain.

Let $\mathcal{T}$ be a triangular mesh of Ω, satisfying the following assumptions :

$$\text{For any angle } \theta \text{ of a triangle of } \mathcal{T}, \text{ one has: } 0 < \theta < \frac{\pi}{2}. \tag{11}$$

There exist $\alpha_1 > 0, \alpha_2 > 0$ and $h > 0$ such that $\forall T \in \mathcal{T}$, and for any edge a of the mesh,

$$\alpha_1 h^2 \leq S(T) \leq \alpha_2 h^2, \text{ and } \alpha_1 h \leq \ell(a) \leq \alpha_2 h, \tag{12}$$

where $S(T)$ denotes the area of triangle T and $\ell(a)$ denotes the length of edge a.

Remark 1 *If the geometry requires a mesh with angles equal to $\frac{\pi}{2}$, a mixture of rectangles and triangles may be used for the discretization; hence assumption (11) is not as restrictive as might seem.*

Using this triangular mesh, a four point finite volume scheme will be defined in section 2.1 for the numerical solution of problem (1)-(2), for which we shall recall an error estimate of order h which was proven in [11].

Equations (3) and (4) express conservation laws and therefore finite volume methods seem to be suitable for a numerical solution (see e.g. [5], [9], [12]). In fact, Equations (9) and (10) form a system of a hyperbolic equation coupled with and elliptic equation. The finite volume method is known to be well adapted to the discretization of non linear hyperbolic conservation laws. Convergence results and error estimates were derived by several authors [3], [16] and [5].

In the case of Equations (9) and (10), Eymard and Gallouët [4] introduced a "weighted finite volume" scheme, which uses both the features of the finite element method and the "classical" finite volume scheme.

A convergence result was obtained in the case where $k_1 + k_2$ depends only on $\mathbf{x}$. We shall also use in the sequel the so called "weighted finite volume scheme" (see also [5]) where the assumption (11) on the mesh may be weakened to :

$$\text{For any angle } \theta \text{ of a triangle of } \mathcal{T}, \text{ one has: } 0 < \theta \leq \frac{\pi}{2}. \tag{13}$$

Using the same triangular mesh, a four point finite volume scheme will be defined in section 2.2 for the numerical solution of problem (9)-(10), (5)-(8) for which the convergence was proven in the case where the function $k_1 + k_2$ does not depend on s [15].

We shall describe both schemes and compare them numerically.

2 The four point finite volume scheme

2.1 The diffusion-convection problem

The principle of the finite volume scheme is to integrate the conservation equation (1) on a control volume T, which yields:

$$-\int_{\partial T} k(\mathbf{x})\nabla u(\mathbf{x}).\mathbf{n}(\mathbf{x})d\sigma(\mathbf{x}) + \int_{\partial T} u(\mathbf{x})\mathbf{v}(\mathbf{x}).\mathbf{n}(\mathbf{x})d\sigma(\mathbf{x}) + \int_T b(\mathbf{x})u(\mathbf{x})d\mathbf{x} = \int_T f(\mathbf{x})d\mathbf{x}, \forall T \in \mathcal{T}, \tag{14}$$

where $\mathbf{n}(\mathbf{x})$ is the outward normal unit vector to the boundary ∂T, and σ is the usual one-dimensional measure on ∂T; next the fluxes need to be approximated on the boundary ∂T of the control volume. Hence we shall approximate the integral of $-k\nabla u.\mathbf{n} + u\mathbf{v}.\mathbf{n}$ over each edge of the mesh. Before we define the numerical scheme, some notations need to be introduced. For $T \in \mathcal{T}$, denote by :

- $S(T)$ the area of triangle T,
- $\mathbf{x}_T$ the intersection of the orthogonal bisectors of the three sides of triangle T,
- $c_i(T)$, $i = 1, 2, 3$, the three sides of triangle T,
- $d(x_T, c_i(T))$ the distance between $\mathbf{x}_T$ and the side $c_i(T)$, for $i = 1, 2, 3$,
- $f_T = \frac{1}{S(T)} \int_T f(\mathbf{x})d\mathbf{x}$ and $b_T = \frac{1}{S(T)} \int_T b(\mathbf{x})d\mathbf{x}$,

and define one discrete unknown per triangle, which will be denoted u_T (located at $\mathbf{x}_T$).

Let $\mathcal{A}$ be the set of the edges of the mesh; $\mathcal{A} = \mathcal{A}_{int} \cup \mathcal{A}_{ext}$, where $\mathcal{A}_{ext} = \mathcal{A} \cap \partial\Omega$ and $\mathcal{A}_{int} = \mathcal{A} \setminus \partial\Omega$; for $a \in \mathcal{A}$, we define:

- $\{u\}_a$ an approximation of u on the edge a ;
- $\mathbf{x}_a$ the center point of edge a.
- $\mathbf{n}_a$ a unit normal vector to the edge a such that $\int_a \mathbf{v}(\mathbf{x}).\mathbf{n}_a d\sigma(\mathbf{x}) \geq 0$;
- $v_a = \frac{1}{\ell(a)} \int_a \mathbf{v}(\mathbf{x}).\mathbf{n}_a d\sigma(\mathbf{x})$;
- if $a \in \mathcal{A}_{int}$, define:

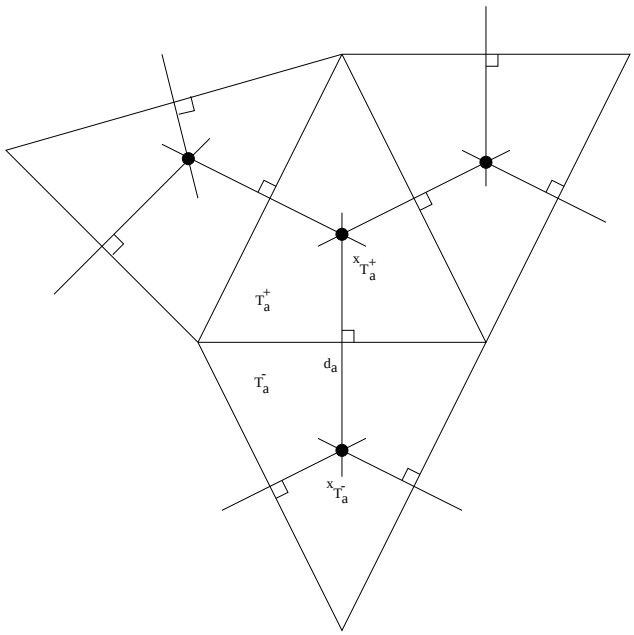

Figure 1: The triangular mesh

* T_a^+ and T_a^- the two triangles for which a is an edge; T_a^+ (resp. T_a^-) is the upstream (resp. downstream) with respect to the convection velocity $\mathbf{v}$, i.e.: such that $\mathbf{n}_a$ is exterior (resp. interior) to T_a^+ (resp. T_a^-).
* $d_a = d(\mathbf{x}_{T_a^+}, a) + d(\mathbf{x}_{T_a^-}, a)$
* Then we can define the "exchange term" at interface a, $E(T_a^+, T_a^-)$, as the approximation of $\int_a k(\mathbf{x})\nabla u(\mathbf{x}).\mathbf{n}(\mathbf{x})d\sigma(\mathbf{x}) + \int_a u(\mathbf{x})\mathbf{v}(\mathbf{x}).\mathbf{n}(\mathbf{x})d\sigma(\mathbf{x})$, by:

$$E(T_a^+, T_a^-) = (-k_a \frac{u_{T_a^-} - u_{T_a^+}}{d_a} + v_a\{u\}_a)\ell(a), \tag{15}$$

where k_a is the value of k at the center of interface a and $\{u\}_a = u_{T_a^+}$ (upstream choice), and $E(T_a^-, T_a^+) = -E(T_a^+, T_a^-)$.
Expression (15) satisfies the two main finite volume principles :

1. Conservation principle : $E(T_a^+, T_a^-) = -E(T_a^-, T_a^+)$,
2. Consistency principle : $-k_a \frac{u_{T_a^-} - u_{T_a^+}}{d_a}$ is a first order approximation of $\int_a k\nabla u.\mathbf{n}$. This is the consequence of the fact that the line $(\mathbf{x}_{T_a^+}, \mathbf{x}_{T_a^-})$ is the orthogonal bisector of edge a.

- If $a \in \mathcal{A}_{ext}$, let
  * g_a be the value of g at the center of interface a,
  * T_a the triangle for which a is an edge. We then set $\{u\}_a$ as the upstream choice : $\{u\}_a = u_{T_a^+}$ if $T_a = T_a^+$, that is if $\mathbf{n}_a$ is exterior to T_a^+, and $\{u\}_a = g_a$ otherwise.

Given the exchange terms, we can now simply define the flux term on an edge $c_i(T)$ for $T \in \mathcal{T}$ and $i \in \{1, 2, 3\}$:

- If $c_i(T) \not\subset \partial\Omega$,

$$F_{T,i} = \begin{cases} \frac{E(T^+_{c_i(T)}, T^-_{c_i(T)})}{\ell(c_i(T))} & \text{if } T = T^+_{c_i(T)} \\ \frac{E(T^-_{c_i(T)}, T^+_{c_i(T)})}{\ell(c_i(T))} & \text{if } T = T^-_{c_i(T)} \end{cases} \tag{16}$$

- If $c_i(T) \subset \partial\Omega$, then

$$F_{T,i} = \begin{cases} -k_{c_i(T)} \frac{g_{c_i(T)} - u_T}{d(x_T, c_i(T))} + v_{c_i(T)} u_{T^+_{c_i(T)}} & \text{if } T = T^+_{c_i(T)} \\ -k_{c_i(T)} \frac{g_{c_i(T)} - u_T}{d(x_T, c_i(T))} - v_{c_i(T)} g_{c_i(T)} & \text{if } T = T^-_{c_i(T)} \end{cases} \tag{17}$$

The numerical scheme for the discretization of equations (1)-(2) is thus:

$$\sum_{i=1}^{3} F_{T,i} \ell(c_i(T)) + S(T) b_T u_T = S(T) f_T, \quad \forall T \in \mathcal{T}. \tag{18}$$

One can show that relations (15) (16), (17) and (18) uniquely define the discrete unknowns $u_T, T \in \mathcal{T}$. The numerical scheme thus defined converges, and the following error estimate holds :

Theorem 1 *Let $(u_T)_{T \in \mathcal{T}}$ be defined by the numerical scheme (15)-(18), $\overline{u}_T = u(\mathbf{x}_T)$ for $T \in \mathcal{T}$, where u denotes the exact solution to problem (1)-(2) and $\mathbf{x}_T$ the intersection of the perpendicular bisectors of triangle T; define the error by : $e_T = u_T - \overline{u}_T$. There exists $C \geq 0$ depending only on u, κ, α_1 and α_2 such that $\left(\sum_{T \in \mathcal{T}} h^2 |e_T|^2\right)^{\frac{1}{2}} \leq Ch$.*

Remark 2 *This estimate shows that the L^2 norm of the error is of order h, since the area of each triangle is of order h^2.*

Furthermore, the numerical scheme satisfies a discrete maximum principle, that is :

Proposition 1 *If $f_T \geq 0$, $\forall T \in \mathcal{T}$, and $g_a \geq 0$, $\forall a \in \mathcal{A}_{ext}$, then the solution $(u_T)_{T \in \mathcal{T}}$ of (15)-(18) satisfies $u_T \geq 0$.*

We refer to [11] for the proof of these results and for references concerning other techniques of proof.

2.2 The elliptic-hyperbolic system

Integrating Equations (9) and (10) over T yields :

$$\int_T s_t(\mathbf{x},t) d\mathbf{x} - \int_{\partial T} k_1(s(\mathbf{x},t)) \nabla u(\mathbf{x},t).\mathbf{n}(\mathbf{x}) d\sigma(\mathbf{x}) = \int_T f_1(\mathbf{x},t) d\mathbf{x}, \forall T \in \mathcal{T}, \tag{19}$$

$$-\int_{\partial T} (k_1 + k_2)(s(\mathbf{x},t)) \nabla u(\mathbf{x},t).\mathbf{n}(\mathbf{x}) d\sigma(\mathbf{x}) = \int_T (f_1 + f_2)(\mathbf{x},t) d\mathbf{x}, \forall T \in \mathcal{T}, \tag{20}$$

where $\mathbf{n}(\mathbf{x})$ is the outward normal unit vector to the boundary ∂T, and σ is the one-dimensional Lebesgue measure on ∂T. We use an explicit scheme on s and an implicit scheme on u for the time discretization of problem (19)-(20). Next the fluxes need to be approximated on the boundary ∂T of the control volume.

Using the notations introduced in section 2.1, define the "exchange terms" at interface a and at time step $n+1$:

- for Equation (19) :

$$E^{n+1}(T_a^+, T_a^-) = -k_1(\{s\}_a) \ell(a) \frac{u^{n+1}_{T_a^-} - u^{n+1}_{T_a^+}}{d_a} \tag{21}$$

and $E^{n+1}(T_a^+, T_a^-) = -E^{n+1}(T_a^-, T_a^+)$

- for Equation (20) :

$$\tilde{E}^{n+1}(T_a^+, T_a^-) = -(k_1 + k_2)(\{s\}_a)\ell(a)\frac{u_{T_a^-}^{n+1} - u_{T_a^+}^{n+1}}{d_a} \tag{22}$$

and $\tilde{E}^{n+1}(T_a^+, T_a^-) = -\tilde{E}^{n+1}(T_a^-, T_a^+)$ (finite volume scheme conservation principle), where $\{s\}_a = s_{T_a^+}^n$ (upstream choice).

Let $T \in \mathcal{T}$ and $i \in \{1, 2, 3\}$, we define the following terms using the same notations as in section 2.1 :

- If $c_i(T) \notin \partial\Omega$,
  - for Equation (19) :

$$F_{T,i}^{n+1} = \begin{cases} \frac{E^{n+1}(T_{c_i(T)}^+, T_{c_i(T)}^-)}{\ell(c_i(T))} & \text{if } T = T_{c_i(T)}^+ \\ \frac{E^{n+1}(T_{c_i(T)}^-, T_{c_i(T)}^+)}{\ell(c_i(T))} & \text{if } T = T_{c_i(T)}^- \end{cases} \tag{23}$$

  - for Equation (20) :

$$\tilde{F}_{T,i}^{n+1} = \begin{cases} \frac{\tilde{E}^{n+1}(T_{c_i(T)}^+, T_{c_i(T)}^-)}{\ell(c_i(T))} & \text{if } T = T_{c_i(T)}^+ \\ \frac{\tilde{E}^{n+1}(T_{c_i(T)}^-, T_{c_i(T)}^+)}{\ell(c_i(T))} & \text{if } T = T_{c_i(T)}^- \end{cases} \tag{24}$$

- If $c_i(T) \subset \partial\Omega$, then
  - for Equation (19) :

$$F_{T,i}^{n+1} = \begin{cases} -k_1(s_{T_a^+}^n)\frac{u_{1,c_i(T)} - u_T^{n+1}}{d(x_T, c_i(T))} & \text{if } T = T_{c_i(T)}^+ \\ -k_1(s_{1,c_i(T)})\frac{u_{1,c_i(T)} - u_T^{n+1}}{d(x_T, c_i(T))} & \text{if } T = T_{c_i(T)}^- \end{cases} \tag{25}$$

  - for Equation (20) :

$$\tilde{F}_{T,i}^{n+1} = \begin{cases} -(k_1 + k_2)(s_{T_a^+}^n)\frac{u_{1,c_i(T)} - u_T^{n+1}}{d(x_T, c_i(T))} & \text{if } T = T_{c_i(T)}^+ \\ -(k_1 + k_2)(s_{1,c_i(T)})\frac{u_{1,c_i(T)} - u_T^{n+1}}{d(x_T, c_i(T))} & \text{if } T = T_{c_i(T)}^- \end{cases} \tag{26}$$

Where $u_{1,c_i(T)}$ is the value of u_1 at the center of interface $c_i(T)$.

The numerical scheme for the discretization of equations (9)-(10) is then:

$$S(T)(s_T^{n+1} - s_T^n) + \Delta t \sum_{i=1}^{3} F_{T,i}^{n+1}\ell(c_i(T)) = S(T)\Delta t(f_1)_T, \quad \forall T \in \mathcal{T}, \tag{27}$$

$$\sum_{i=1}^{3} \tilde{F}_{T,i}^{n+1}\ell(c_i(T)) = S(T)(f_1 + f_2)_T, \quad \forall T \in \mathcal{T}, \tag{28}$$

where :

- Δt is the time step,
- $(f_1)_T = \int_T f_1(\mathbf{x}, t^n)d\mathbf{x}$ with $t^n = n\Delta t$,
- $(f_1 + f_2)_T = \int_T (f_1 + f_2)(\mathbf{x}, t^n)d\mathbf{x}$ with $t^n = n\Delta t$,
- $s_T^n \in \mathbb{R}$ is an approximation of s on triangle T at time t^n.

Remark 3 *In the case where $k_1 + k_2$ depends only on $\mathbf{x}$ and t but not on s, it was recently proven (see [15]) that the numerical scheme thus defined is convergent.*

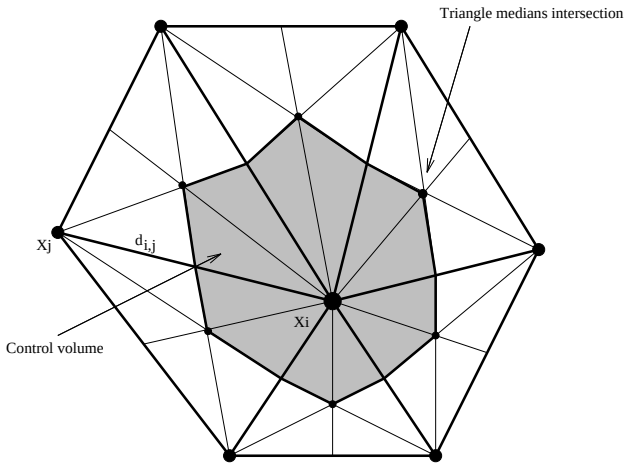

Figure 2: Control volume

3 The weighted finite volume scheme

Recent methods were developped to try and profit from the advantages of both finite element and finite volume methods [4], [8]. We shall use here the method of "weighted finite volumes" [4], which treats the diffusion terms with a finite element method and the convection terms with a finite volume method.

3.1 The diffusion-convection problem

The principle of weighted finite volume scheme on a triangular mesh (see e.g. [4]), is similar to the linear finite element framework, in that a weak formulation of Equation (1) is considered :

$$\int_\Omega k(\mathbf{x})\nabla u(\mathbf{x})\nabla\varphi(\mathbf{x})d\mathbf{x} - \int_\Omega u(\mathbf{x})\mathbf{v}(\mathbf{x})\nabla\varphi(\mathbf{x})d\mathbf{x} + \int_\Omega b(\mathbf{x})u(\mathbf{x})\varphi(\mathbf{x})d\mathbf{x} = \int_\Omega f(\mathbf{x})\varphi(\mathbf{x})d\mathbf{x}, \forall\varphi \in C_c^\infty(\Omega), \tag{29}$$

Hence we shall approximate the integral of $k\nabla u\nabla\varphi - u\mathbf{v}.\nabla\varphi + bu\varphi$ over Ω. Before we define the numerical scheme, some notations need to be introduced.

Assume that $\mathbf{v}$ satisfies the following assumption :

$$\text{There exists } p \in C^2(\overline{\Omega}, \mathbb{R}) \text{ such that } \forall\mathbf{x} \in \overline{\Omega}, \mathbf{v}(\mathbf{x}) = \nabla p(\mathbf{x}) \tag{30}$$

Denote by :

- $\mathcal{I}$ the set of the nodes of the mesh, $\mathcal{I}_{ext} = \mathcal{I} \cap \partial\Omega$, $\mathcal{I}_{int} = \mathcal{I} \setminus \partial\Omega$,
- M (resp. M_{ext}, M_{int}) the number of nodes in $\mathcal{I}$ (resp. $\mathcal{I}_{ext}, \mathcal{I}_{int}$),
- $u_i \in \mathbb{R}$ an approximation of u at the node i, for $i = 1, \cdots, M$,
- $p_i \in \mathbb{R}$ an approximation of p at the node i, for $i = 1, \cdots, M$,
- φ_i the linear finite element shape function relative to the node i,
- $\mathbf{x}_i$ the location of the node i,
- $f_i = \int_\Omega f(\mathbf{x})\varphi_i(\mathbf{x})d\mathbf{x}$,

- $b_{i,j} = \int_\Omega b(\mathbf{x})\varphi_i(\mathbf{x})\varphi_j(\mathbf{x})d\mathbf{x}$,
- $K_{i,j} = \int_\Omega \nabla\varphi_i(\mathbf{x}).\nabla\varphi_j(\mathbf{x})d\mathbf{x}$,
- $\tilde{K}_{i,j} = \int_\Omega k(\mathbf{x})\nabla\varphi_i(\mathbf{x}).\nabla\varphi_j(\mathbf{x})d\mathbf{x}$,

Remark 4 *The linear finite element shape function ψ_i relative to a node i of $\mathcal{T}$ satisfies:*

$$\int_T \psi_i \ \partial\Omega = \frac{1}{3}S(T) \tag{31}$$

where $T \in \mathcal{T}$ and $S(T)$ is the area of triangle T.
We use a Galerkin decomposition of u and p on the linear finite element shape functions and define u_h and p_h by:

$$u_h(\mathbf{x}) = \sum_{j=1}^{M} u_j\varphi_j(\mathbf{x}), \tag{32}$$

$$p_h(\mathbf{x}) = \sum_{j=1}^{M} p_j\varphi_j(\mathbf{x}), \tag{33}$$

where h represents the "size" of the mesh $\mathcal{T}$, satisfying assumptions (12)-(13). A general interpolation result yields for $u_i = u(\mathbf{x}_i)$, $p_i = p(\mathbf{x}_i)$, $\forall i \in \mathcal{I}$ (see e.g. [2]) :

$$\|u - u_h\|_{L^2(\Omega)} \leq C_1.h \tag{34}$$

$$\|p - p_h\|_{L^2(\Omega)} \leq C_2.h \tag{35}$$

Using the Galerkin approximation of u in the terms $\int_\Omega k(\mathbf{x})\nabla u.\nabla\varphi_i dx$, $\int_\Omega bu\varphi_i dx$ and $\int_\Omega f\varphi_i dx$ in Equation (29) yields $\sum_j \tilde{K}_{i,j}u_j$, $\sum_j b_{i,j}u_j$ and f_i. The convective term $\int_\Omega uv\nabla\varphi_i dx$ is approximated by using the Galerkin approximation of $v = \nabla p$. Note that no Galerkin development is used for u. Rather, remark that :

$$\sum_{j\in\mathcal{I}_{int}} p_j\nabla\varphi_i\nabla\varphi_j = \sum_{\substack{j\in\mathcal{I}_{int}\\ j\neq i}} (p_j - p_i)\nabla\varphi_i\nabla\varphi_j, \forall i \in \mathcal{I}_{int} \tag{36}$$

Hence, the approximated convected term $\int_\Omega \sum_{\substack{j\in\mathcal{I}_{int}\\ j\neq i}} (p_j - p_i)\nabla\varphi_i\nabla\varphi_j$ may be seen as a sum of exchange terms between nodes i and j, and a reasonable choice for u seems to be the following "upstream" choice :

$$\{u\}_{i,j} = \begin{cases} u_i & \text{if } p_i - p_j > 0 \\ u_j & \text{if } p_i - p_j < 0 \end{cases} \tag{37}$$

Hence,the following "weighted finite volume" scheme :

$$\sum_{j\in\mathcal{I}_{int}} u_j\tilde{K}_{i,j} - \sum_{\substack{j\in\mathcal{I}_{int}\\ j\neq i}} \{u\}_{i,j}(p_j - p_i)K_{i,j} + \sum_{j\in\mathcal{I}_{int}} u_j b_{i,j} = f_i, \forall i \in \mathcal{I}_{int} \tag{38}$$

Note that in the case of a pure diffusion operator, i.e. $\mathbf{v} = 0$, the above system is the discrete system obtained by the classical piecewise linear finite element method.

3.2 The elliptic-hyperbolic system

Let us now consider a weak formulation of Equations (9) and (10) :

$$\int_\Omega s_t(\mathbf{x},t)\varphi(\mathbf{x})d\mathbf{x} + \int_\Omega k_1(s(\mathbf{x},t))\nabla p(\mathbf{x},t).\nabla\varphi(\mathbf{x})d\mathbf{x} = \int_\Omega f_1(\mathbf{x},t)\varphi(\mathbf{x})d\mathbf{x}, \forall\varphi\in C_c^\infty(\Omega) \quad (39)$$

$$\int_\Omega (k_1+k_2)(s(\mathbf{x},t))\nabla p(\mathbf{x},t).\nabla\varphi(\mathbf{x})d\mathbf{x} = \int_\Omega (f_1+f_2)(\mathbf{x},t)\varphi(\mathbf{x})d\mathbf{x}, \forall\varphi\in C_c^\infty(\Omega) \quad (40)$$

We use an explicit scheme on s and an implicit scheme on p for the time discretization of problem (39)-(40). Before we define the numerical scheme, some notations need to be introduced. Using the same notations as above for the space discretization, define :

- Δt the time step,
- $t^n = n\Delta t$, $n\in\mathbb{N}$,
- $p_i^n\in\mathbb{R}$ an approximation of p at the node i and at time step n, for $i=1,\cdots,M$,
- $s_i^n\in\mathbb{R}$ an approximation of s at the node i and at time step n, for $i=1,\cdots,M$,
- $f_i^n = \int_\Omega f_1(\mathbf{x},t^n)\varphi_i(\mathbf{x})d\mathbf{x}$,
- $\tilde{f}_i^n = \int_\Omega (f_1+f_2)(\mathbf{x},t^n)\varphi_i(\mathbf{x})d\mathbf{x}$,
- $K_{i,j} = \int_\Omega \nabla\varphi_i(\mathbf{x}).\nabla\varphi_j(\mathbf{x})d\mathbf{x}$,

We use a Galerkin decomposition of p on the linear finite element shape functions and define p_h^n by:

$$p_h^n(\mathbf{x}) = \sum_{j=1}^M p_j^n\varphi_j(\mathbf{x}) \quad (41)$$

where h represents the "size" of the mesh $\mathcal{T}$, satisfying assumptions (12)-(13). Similarly as in the convection-diffusion case, let us define $\{s\}_{i,j}$ an upstream approximation of s, on the edge defined by the i and j nodes, by :

$$\{s\}_{i,j}^n = \begin{cases} s_i^n & \text{if } p_i^n - p_j^n > 0 \\ s_j^n & \text{if } p_i^n - p_j^n < 0 \end{cases} \quad (42)$$

Then, using the Galerkin decomposition (41) on p, the terms $\int_\Omega k_1(s(\mathbf{x},t^n))\nabla p(\mathbf{x},t^n).\nabla\varphi_i(\mathbf{x})d\mathbf{x}$ of Equation (39) and $\int_\Omega (k_1+k_2)(s(\mathbf{x},t^n))\nabla p(\mathbf{x},t^n).\nabla\varphi_i(\mathbf{x})d\mathbf{x}$ of Equation (40) ($i\in\mathcal{I}_{int}$) are approximated respectively by:

$$F_i^{n+1} = \sum_{\substack{j\in\mathcal{I}_{int}\\ j\neq i}} k_1(\{s\}_{i,j}^n)(p_j^{n+1}-p_i^{n+1})K_{i,j}\,, \quad (43)$$

$$\tilde{F}_i^{n+1} = \sum_{\substack{j\in\mathcal{I}_{int}\\ j\neq i}} (k_1+k_2)(\{s\}_{i,j}^n)(p_j^{n+1}-p_i^{n+1})K_{i,j}\,. \quad (44)$$

Therefore, using an Euler explicit scheme on s and relation (31), the following numerical scheme is obtained:

$$|Supp(\varphi_i)|(s_i^{n+1}-s_i^n) + 3\Delta t.F_i^{n+1} = 3\Delta t.f_i^n, \quad \forall i\in\mathcal{I}_{int}, \quad (45)$$

$$\tilde{F}_i^{n+1} = \tilde{f}_i^n, \quad \forall i\in\mathcal{I}_{int}, \quad (46)$$

where $|Supp(\varphi_i)|$ denotes the area of the support of the test function φ_i.

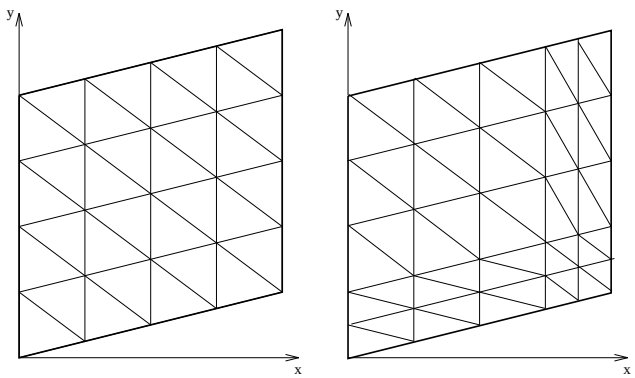

Figure 3: Mesh definition and local mesh refinement

Remark 5 *In the case where $k_1 + k_2$ only depends on* $\mathbf{x}$ *and t but not on s, one can show that the numerical scheme thus defined is convergent (see [4]).*

4 Numerical results

We now describe a series of numerical tests which were performed in order to compare the two schemes.

Consider the following pure diffusion problem :

$$-\Delta u(x_1, x_2) = -4\pi^2 x_2 sin(2\pi x_1), (x_1, x_2) \in \Omega, \quad (47)$$

$$u(x_1, x_2) = x_2 sin(2\pi x_1), (x_1, x_2) \in \partial\Omega, \quad (48)$$

where Ω is a parallelogram defined on Figure 3.

The domain Ω is discretized with a triangular mesh (see fig 3).
We shall compare the performance of the finite volume scheme described in section (2.1) with the weighted finite volume scheme which is, in the case of Equations (47)-(48), the piecewise linear finite element method. First numericals tests are performed in order to study the behaviour of the finite volume scheme when some of the angles of the mesh tend to $\frac{\pi}{2}$ (recall that the condition $0 < \theta < \frac{\pi}{2}$ is necessary for the error estimate, but that this error estimate does not depend on $inf_\theta\{(\frac{\pi}{2} - \theta)\}$).

It can be noticed from the results of Figure 4 that the approximation error increases as the maximum angle of the mesh tends to $\frac{\pi}{2}$. However, the error remains bounded. The condition number of the linear system to be solved increases, which leads to numerical difficulties in the linear system solver.

Let us now define the discrete norms which will be used in the comparative tests:

- In the case of the finite element scheme; let $u_\mathcal{T}$ denote the piecewise linear finite element approximation to the solution; then the approximation error $e^{FE} = u - u_\mathcal{T}$ is a function of $H^1(\Omega)$, and one may therefore easily define its L^2 and H_0^1 norm as :

$$\|e^{FE}\|_{L^2} = (\int_\Omega (u(\mathbf{x}) - u_\mathcal{T}(\mathbf{x}))^2 d\mathbf{x})^{\frac{1}{2}}, \quad (49)$$

$$\|e^{FE}\|_{H_0^1} = (\int_\Omega \mid \nabla u(\mathbf{x}) - \nabla u_\mathcal{T}(\mathbf{x}) \mid^2 d\mathbf{x})^{\frac{1}{2}}, \quad (50)$$

- In the case of the finite volume scheme, the approximation error can be expressed as a piecewise constant function e^{FV} from Ω to $\mathbb{R}$ where the value of e^{FV} on a given triangle $T \in \mathcal{T}$ of the mesh

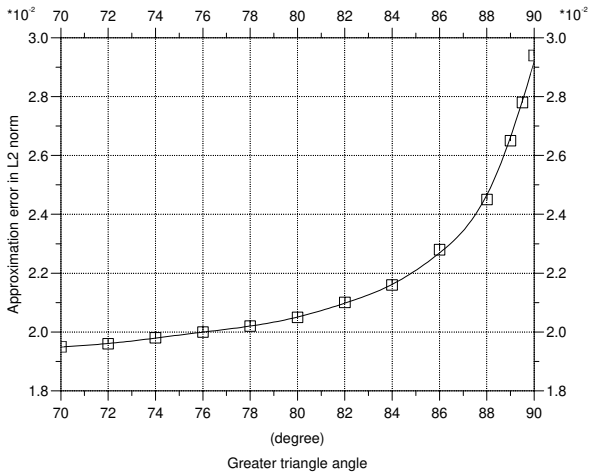

Figure 4: Finite Volume scheme behavior on a limit case, pure diffusion case, Problem (47)-(48).

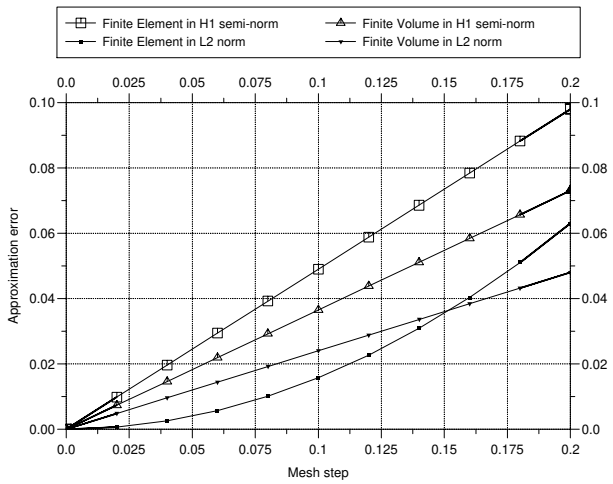

Figure 5: Finite Volume, Finite Element comparison, pure diffusion case, Problem (47)-(48).

is constant and given by: $e_T^{FV} = u(\mathbf{x}_T) - u_T$. The L^2 norm of the approximation error e^{FV} is then defined by:

$$\|e^{FV}\|_{L^2} = h(\sum_{T \in \mathcal{T}} (e_T^{FV})^2)^{\frac{1}{2}}, \tag{51}$$

We define a "discrete H_0^1" norm as :

$$\|e^{FV}\|_{H_0^1} = (\sum_{a \in \mathcal{A}} |e_{T_a^+}^{FV}) - e_{T_a^-}^{FV}|^2)^{\frac{1}{2}}, \tag{52}$$

The L^2 and H_0^1 norm of the approximation error are plotted vs the mesh size in Figure 5. As expected, the finite element L^2 norm of the error shows a quadratic performance, while the finite volume L^2 norm increases linearly with the mesh size (this is in agreement with Theorem 1). The H_0^1 norm of the approximation error of both schemes behaves linearly.

The L^2 norm of the approximation error of both schemes are plotted vs the CPU time in Figure 6. The data

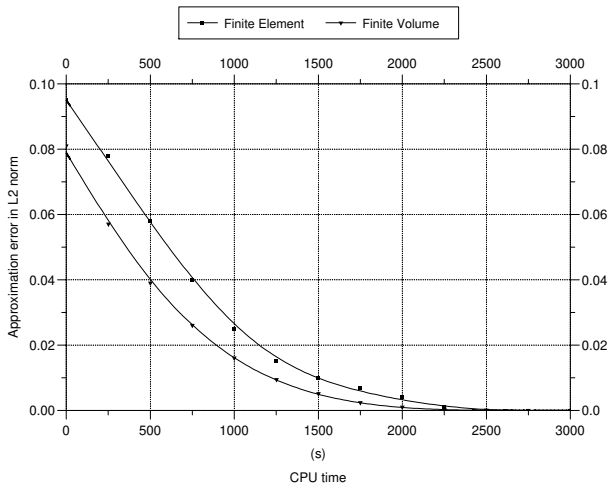

Figure 6: Finite Volume, Finite Element CPU time comparison, pure diffusion case, Problem (47)-(48).

structure of the finite element code is more complex than that of the finite volume code for the solution of the same problem. This explains the somewhat lower efficiency of the finite element code.

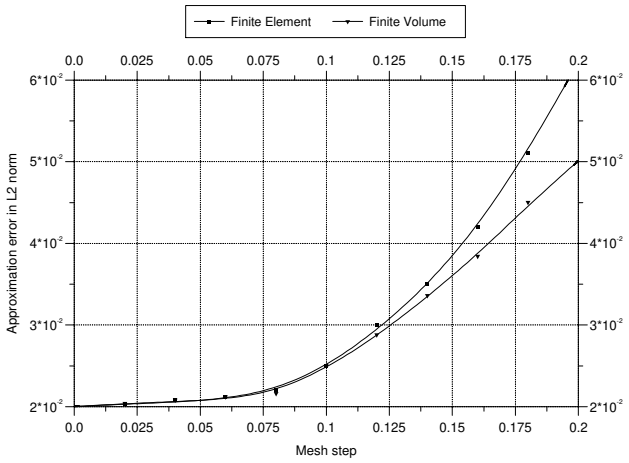

Figure 7: Finite Volume, Finite Element comparison on locally refined mesh, pure diffusion case, Problem (47)-(48).

Figure 7 shows the behavior of the approximation error on the finite element and finite volume schemes when the first line and the last column of the mesh are refined (see Figure 3). When the refinement step tends to zero, the two schemes behave similarly as seen on Figure 7.

Figure 8 shows the precision of the approximation of the fluxes for the finite element and finite volume scheme with respect to the mesh size. It is clear from the results that the finite volume scheme gives a more precise approximation of the flux. This may be of importance in certain coupled problems (see e.g. [7]).

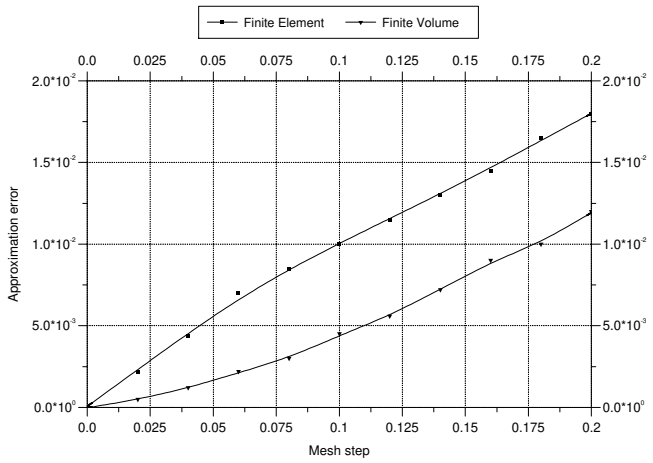

Figure 8: Finite Volume, Finite Element comparison on fluxes, pure diffusion case, Problem (47)-(48).

4.1 Four point finite volume scheme versus weighted finite volume scheme on a diffusion-convection problem

Consider the following diffusion-convection problem :

$$
\begin{aligned}
div(u(x_1,x_2)\nabla P(x_1,x_2)) - \Delta u(x_1,x_2) &= (6x_1^2-2)e^{x_2}, (x_1,x_2) \in \Omega, &(53)\\
u(x_1,x_2) &= x_1^2 e^{x_2}, (x_1,x_2) \in \partial\Omega, &(54)\\
P(x_1,x_2) &= x_1^2 + x_2, (x_1,x_2) \in \Omega, &(55)
\end{aligned}
$$

where Ω is a parallelogram defined on Figure 3, which is discretized with an irregular triangular mesh.

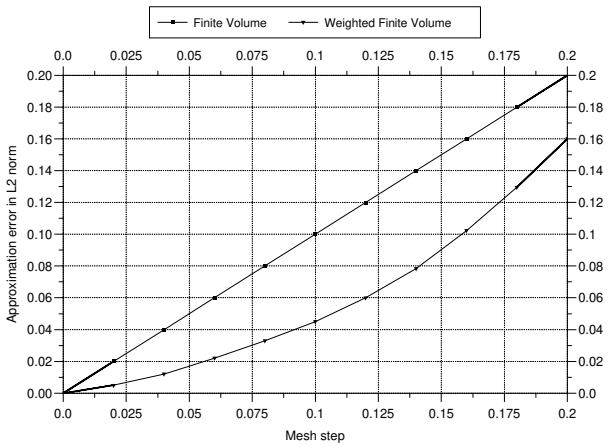

Figure 9: Finite Volume, Weighted Finite Volume comparison, convection-diffusion case, Problem (53)-(55).

Figure 9 shows the approximation error for the finite volume and weighted finite volume discretizations of problem (53)-(55). The approximation error of the convection term is (theoretically) of order 1 with respect to the mesh size for both methods. The diffusion term is better approximated by the weighted finite volume

scheme. The quadratic behaviour is indeed observed for coarse meshes, whereas a quasi-linear behaviour is found for fine meshes.

4.2 Case of a nonlinear hyperbolic equation

Consider the following nonlinear hyperbolic equation in two space dimensions :

$$\begin{aligned} u_t(x_1,x_2,t) + div(f(u)\nabla p(x_1,x_2)) &= 2t + 2(x_1+x_2)(x_1x_2+t^2), ((x_1,x_2),t) \in \Omega\times]0,T[, & (56)\\ u(x_1,x_2,t) &= x_1x_2+t^2, ((x_1,x_2),t) \in \partial\Omega\times]0,T[, & (57)\\ u(x_1,x_2,0) &= x_1x_2, (x_1,x_2) \in \Omega, & (58) \end{aligned}$$

where $\Omega \subset \mathbb{R}^2$ is a parallelogram defined on Figure 3, discretized with an irregular triangular mesh, and f and p are defined by:

$$\begin{aligned} f(u) &= u^2, & (59)\\ p(x_1,x_2) &= x_1+x_2, (x_1,x_2) \in \Omega, & (60) \end{aligned}$$

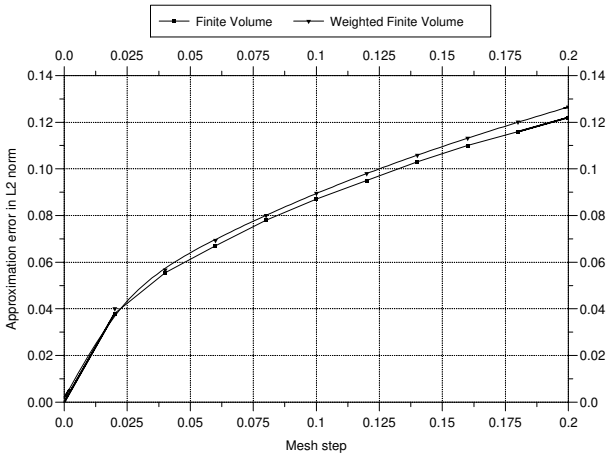

Figure 10: Finite volume, weighted finite volume comparison, hyperbolic case, Problem (56)-(58).

Figure 10 shows the approximation error with respect to the mesh size for both finite volume and weighted finite volume scheme. the behaviour of the error for both schemes is again of order $h^{1/2}$. Note that the theoretical error estimates give an order of $h^{1/4}$

The schemes FV and WVF are similar when implemented on the one-dimensional Burgers equation; in fact, they are similar if a unifom mesh is used. They were both implementd for a Riemann problem yielding a shock propagation. Both schemes show an approximation error of order $h^{\frac{1}{2}}$.

One may add a one dimensional Van Leer procedure for the computation of the fluxes in the direction orthogonal to the edges of the mesh. This method was succesfully used in [1] for the Euler equations. When implemented for the Burgers equation, a decrease of the error of up to 50 percent is obtained.

4.3 Case of an elliptic-hyperbolic coupled system

Consider the following elliptic-hyperbolic coupled system, which models the flow of oil and water through a porous medium, including the gravity effect:

$$
\begin{aligned}
s_t(\mathbf{x},t) - \mathrm{div}(\frac{s(\mathbf{x},t)}{\mu_w}(\nabla p(\mathbf{x},t) - \rho_w \vec{g})) &= 0, (\mathbf{x},t) \in \Omega \times]0,\mathcal{T}[, && (61)\\
-s_t(\mathbf{x},t) - \mathrm{div}(\frac{1-s(\mathbf{x},t)}{\mu_o}(\nabla p(\mathbf{x},t) - \rho_o \vec{g})) &= 0, (\mathbf{x},t) \in \Omega \times]0,\mathcal{T}[, && (62)\\
s(\mathbf{x},t) &= s_1(\mathbf{x},t), (\mathbf{x},t) \in \partial\Omega \times]0,\mathcal{T}[, && (63)\\
s(\mathbf{x},0) &= s_0(\mathbf{x}), \mathbf{x} \in \Omega, && (64)\\
p(\mathbf{x},t) &= p_1(\mathbf{x},t), (\mathbf{x},t) \in \partial\Omega \times]0,\mathcal{T}[, && (65)\\
u(\mathbf{x},0) &= u_0(\mathbf{x}), \mathbf{x} \in \Omega, && (66)
\end{aligned}
$$

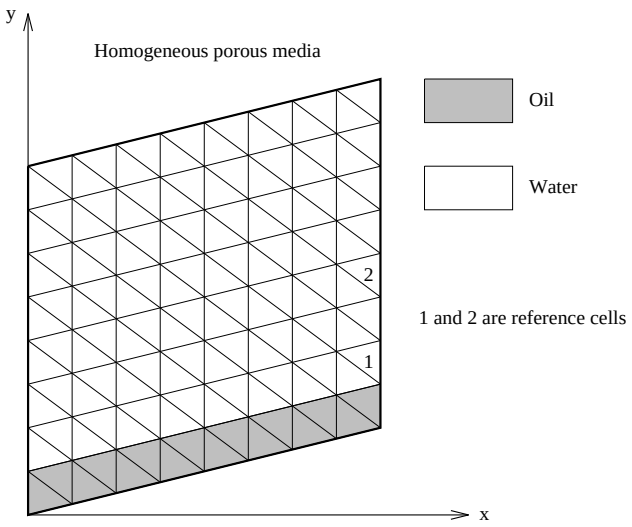

Figure 11: Mesh definition for comparisons

where Ω is a parallelogram defined on Figure 11, $\vec{g}$ is the gravity acceleration vector and μ_w, μ_o (respective viscosities of water and oil), ρ_w and ρ_o (respective densities of water and oil) are given constants. In this case, $(k_1 + k_2)(s) = \frac{s}{\mu_w} + \frac{1-s}{\mu_o}$, so $(k_1 + k_2)$ depends on s. Note that s represents the water phase saturation and p the two phases pressure. The domain Ω is discretized with an irregular triangular mesh (see Fig 11). The "exact" solution was computed using a very fine mesh and a Fujitsu supercomputer, using both schemes, and the results are equal up to the machine precision.

In Figures 12, results for the upwind choice for both schemes are presented. The order of the approximation is $h^{1/2}$ in both cases, but the finite volume scheme is somewhat more precise. Figure 13 shows the results for a Van Leer approximation of the flux (as described in the preceding paragraph in both schemes. The approximation error is much lower for both schemes; it can be noticed that the improvement is best for the weighted finite volume scheme, which is in agreement with the fact that numerical diffusion of weighted finite volume is larger than that of finite volume.

We now present a study of the saturation with respect to the time. We start with a discontinuous saturation: we take $s = 1$ in the shaded cells of Figure 11 and $s = 0$ elsewhere. We shall study the values of the saturation in cells 1 and 2 defined in Figure 11. Figures 14 and 15 show that the results given by both schemes are comparable, and that the Van Leer approximation reduces the numerical diffusion.

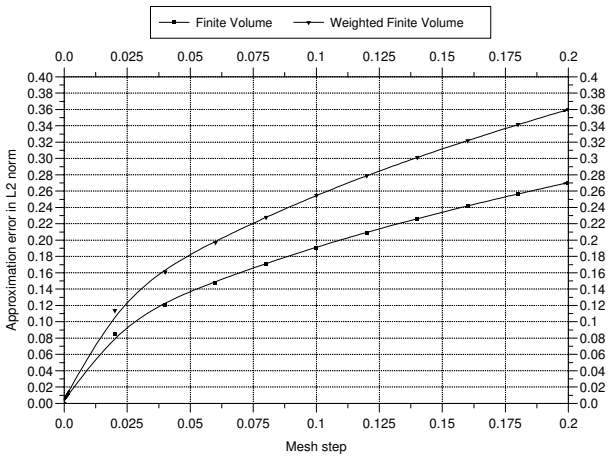

Figure 12: Comparison with an upstream scheme, coupled system case, Problem (61)-(66).

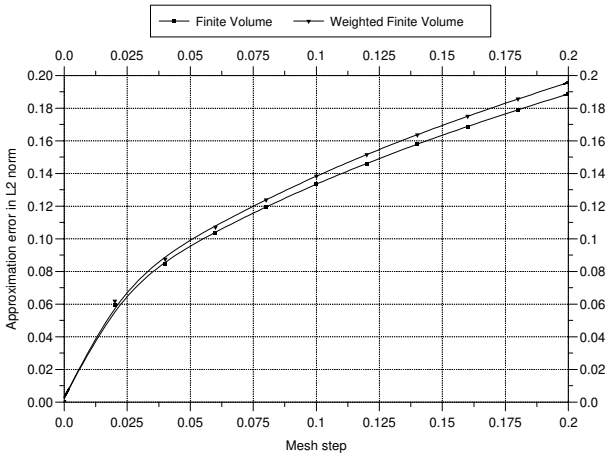

Figure 13: Comparison with a Van-Leer scheme, coupled system case, Problem (61)-(66).

Figure 16 shows that the finite volume scheme is computationally cheaper for a given precision.

A local refinement of the mesh (in a similar as described on Figure 3) is then performed; the finite volume scheme remains more precise in that case (see Figure 17).

In Figure 18 the error on the fluxes is shown. Again they are better approximation with finite volume.

Figure 19 and 20 show the distribution of the approximation error at final time $T = T_{final}$ for both schemes. It can be remarked that the error for the finite volume scheme is higher near the boundaries while it is more uniformly distributed in the case of weighted finite volume.

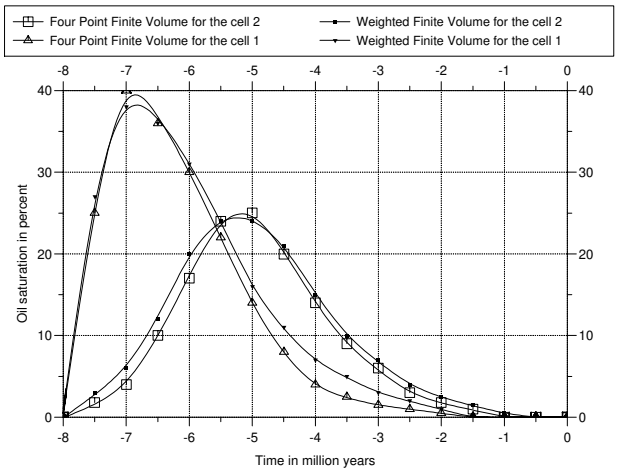

Figure 14: Saturation comparison with an upstream scheme, coupled system case, Problem (61)-(66).

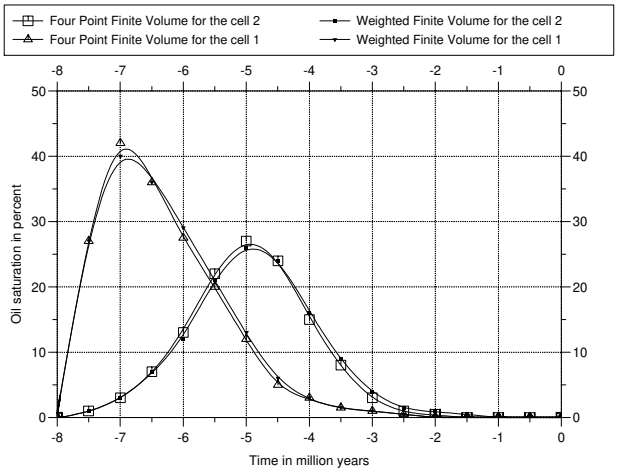

Figure 15: Saturation comparison with a Van Leer scheme, coupled system case, Problem (61)-(66).

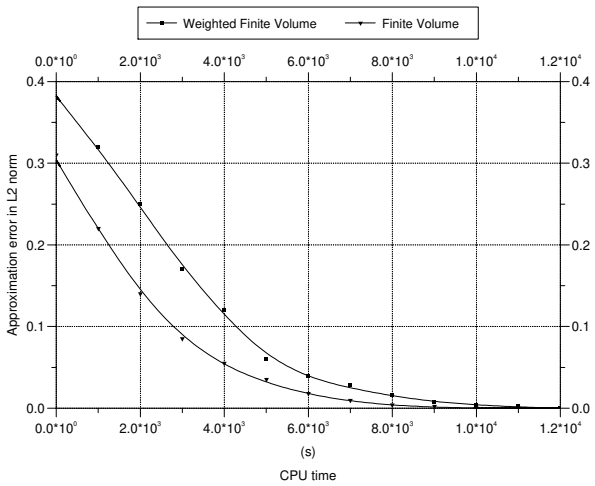

Figure 16: Finite Volume, Weighted Finite Volume CPU time comparison, coupled system case, Problem (61)- (66).

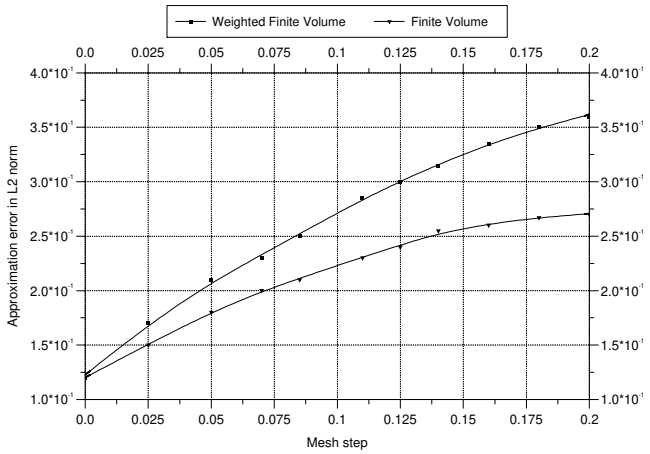

Figure 17: Finite volume, weighted finite volume comparison on locally refined mesh, coupled system case, Problem (61)-(66).

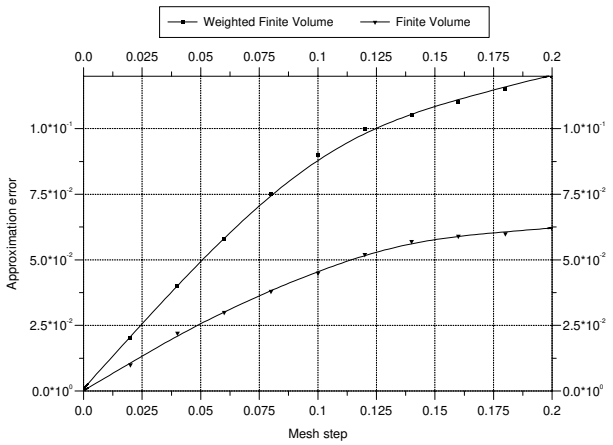

Figure 18: Finite volume, weighted finite volume comparison on fluxes, coupled system case, Problem (61)-(66).

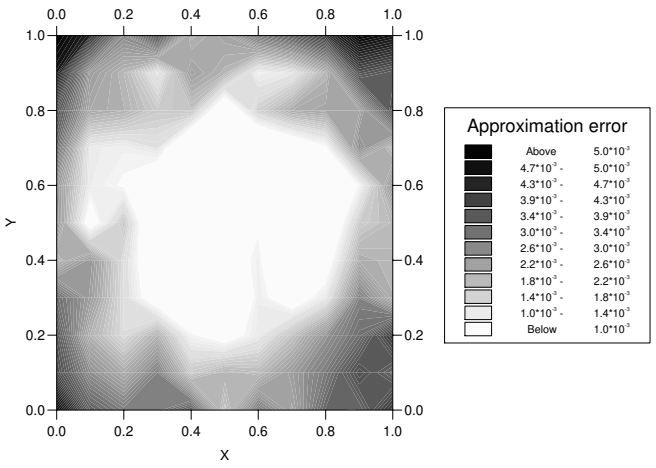

Figure 19: Approximation error for four point finite volume scheme, coupled system case, Problem (61)-(66).

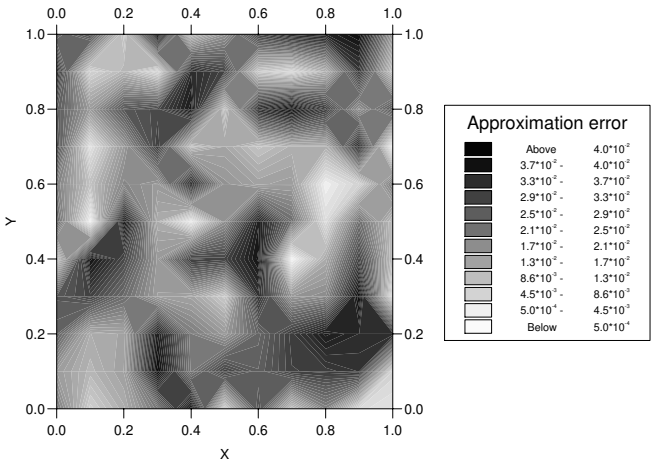

Figure 20: Approximation error for weighted finite volume scheme, coupled system case, Problem (61)-(66).

5 Conclusions

We studied the numerical performance of two finite volume schemes using a triangular mesh for elliptic and hyperbolic equations, and also for a system consisting of a hyperbolic and an elliptic equation. The first scheme is a classical finite volume scheme which uses the othogonal bisectors of the sides of the triangle for the definition of the numerical diffusion flux with respect to the discrete unknowns, located at the intersection of the orthogonal bisectors. The domain of study is discretized with triangles with angles strictly less than $\frac{\pi}{2}$. The approximation of the convection flux is performed on each edge of the mesh by selecting the upwind choice of the given unknown. This four point scheme is easy to implement for elliptic equations and generalizes quite well to the case of parabolic equations (in fact, the error estimate proven in [11] for a stationary problem is also expected to hold for a time implicit scheme of the associate evolution problem). It was also implemented in the case of a nonlinear hyperbolic conservation law, and for a system consisting of a Laplace-type equation coupled with a hyperbolic equation.

The second scheme considered is a "weighted finite volume scheme" which was first introduced by [4] for the system above mentionned. This scheme can also be seen as a finite volume scheme defined on a "dual mesh". In the case of the Laplace equation, the weighted finite volume scheme is equivalent to the classical piecewise linear finite element method.

Both schemes were tested numerically for the discretization of the above mentionned equations, in some cases with a local refinement of the mesh. The approximate solution was compared to the analytical solution, when known, and to a numerical solution obtained for a very fine mesh otherwise. The numerical results show that both schemes are well adapted for the discretization of elliptic and hyperbolic equations, and also for mixed problems. Denoting by h the "discretization step", the approximation error is of order h (resp. h^2) for the four point finite volume (resp. weighted finite volume) scheme, in the case of a pure diffusion operator; this is in agreement with the theory. In the case of a nonlinear hyperbolic equation, both schemes show an approximation error of $\sqrt{h}$. This is in fact better than the actual state of the error estimates which have been proven for triangular discretizations up to now, and which are of order $h^{\frac{1}{4}}$ ([3], [16], [5]). Note that in the case of a discretization with rectangles, theoretical error estimates are of order $h^{\frac{1}{2}}$.

The four point scheme is somewhat computationally cheaper and it yields a better approximation of the normal fluxes to the edges of the mesh. The difference between the approximation of the fluxes by the two schemes tends to decrease when a higher order Van Leer scheme is used. This is due mainly to the fact that the numerical diffusion of the weighted finite volume scheme is larger than that of the four point finite volume scheme.

Further work concerns the study of the four point finite volume scheme when the condition on the angles of the mesh is relaxed. In this case, the orthocenter, i.e. the intersection of the orthogonal bisectors, of one given triangle may be located outside of this triangle. However, the error estimate of [11] should still hold provided that the distance between the orthocenters of two neighbouring triangles are of order h, and that no orthocenter lies outside of the domain of study. A preliminary numerical implementation for a simple case suggests that the scheme behaves well even in the case of angles greater than $\frac{\pi}{2}$.

Note that both four point finite volume and weighted finite volume schemes behave well in the case where the scalar diffusion coefficient is replaced by a symmetric positive definite matrix. The case where this matrix is discontinuous at interfaces of the domain (e.g. in the case of a heterogeneous medium) is under study.

References

[1] Chevrier P. Galley H.:A Van Leer finite volume scheme for the Euler equations on unstructured meshes, M^2AN, 27,2, 183-201, 1993.

[2] Ciarlet P.G.: The Finite Element Method for Elliptic Problems. North-Holland, Amsterdam, 1978.

[3] Cockburn B., Coquel F., Le Floch P., An error estimate for high order accurate finite volume methods for scalar conservation laws, to appear in Math. Comput.

[4] Eymard R., Gallouët T.: Convergence d'un Schéma de type Eléments Finis - Volumes Finis pour un Système Couplé Elliptique - Hyperbolique, M2AN, 27, 7, 843-861, 1993.

[5] Eymard R., Gallouët T. and Herbin R., The finite volume method, in preparation for the "Handbook of Numerical Analysis", Ph. Ciarlet et J.L. Lions eds.

[6] Faille I. A control volume method to solve an elliptic equation on a 2D irregular meshing, Comp. Meth. Appl. Mech. Engrg., 100, 275 (1992).

[7] Fiard J.M., Herbin R., Comparison between finite volume and finite element methods for the numerical simulation of an elliptic problem arising in electrochemical engineering, Comput. Meth. Appl. Mech. Engin. 115, 315-338, 1994.

[8] Forsyth P.A., A control volume finite element method for local mesh refinement, SPE 18415, 85-96, 1989.

[9] Forsyth P.A., A control volume finite element approach to NAPL groundwater contamination, SIAM J. Sci. Stat. Comput., 12, 5, 1029-1057, 1991.

[10] Fezoui L., Lanteri S., Larrouturou B., Olivier C. : Résolution Numérique des Equations de Navier-Stokes pour un Fluide Compressible en Maillage Triangulaire, INRIA report, 1989.

[11] Herbin R., An error estimate for a finite volume scheme for a diffusion convection problem on a triangular mesh, Num. Meth. P.D.E., 165-173, 1995.

[12] Patankar S.V. : Numerical Heat Transfer and Fluid Flow, Series in Computational Methods in Mechanics and Thermal Sciences, Minkowycz and Sparrow Eds., Mc Graw Hill, 1980.

[13] Selmin V. : The node-centred finite volume approach: Bridge between finite differences and finite elements, Comp. Meth. in Appl. Mech. Engin., 102, 107-138, 1993.

[14] Sonier F., Eymard R., Mathematical and numerical properties of control-volume finite-element scheme for reservoir simulation, paper SPE 25267 presented at the 12th symposium on reservoir simulation, New Orleans, 1993.

[15] Vignal M.H., Convergence of a finite volume scheme for a system of an elliptic equation and a hyperbolic equation, accepted for publication in M^2AN.

[16] Vila J.P., Convergence and error estimate in finite volume schemes for general multidimensional conservation laws, I. explicit monotone schemes," M2AN, 28, 267 (1994).